

# Measurement of liquid film behavior of two phase slug flow inside microscale rectangle tube

47-186829 Li Zhaoyu  
Supervisor: Asso Prof. Dang Chaobin

Flow boiling heat transfer in microscale channel can provide very high heat transfer coefficients and are highly compact with a high surface to volume ratio. The dominant heat conduction through thin liquid film vaporization at the liquid-vapor interface is important in the heat transfer characteristics, flow boiling instabilities also depends on the thickness of the liquid film variation. The liquid film thickness measurement was carried out for two phase flow under isothermal conditions in several types glass tubes. The study is enabled through development of a novel device which enables synchronized measurement of liquid film thickness, as well as flow regime observation and pressure drop and void fraction.

Key words: Slug flow, Liquid film thickness, Pressure drop, microchannels

## 1 Introduction

Flow boiling in micro channels has been studied extensively. In microchannels, vapor bubble growth is restricted by the channel wall, and elongated vapor bubbles are confined by liquid slugs and liquid film. This flow regime is defined as slug flow. It is reported that the liquid film thickness is one of the important parameters for predicting boiling heat transfer in micro channel slug flows. For the pioneer study, Youshinaga (2014) measured the initial liquid film thickness in micro circular tubes with laser focus displacement meter. [1]

Compared with the circular tube studies, researches on the square channel two-phase flows are still limited. Kolb and Cerro (1991) used sequential particle tracking techniques to investigate the coating thickness of the liquid deposited on the square channel wall. It is observed that the transition from a non-axisymmetric to axisymmetric bubble occur at  $Ca=0.1$ . [2]

Hydrodynamics of square channel slug flows are thus quite different from those of circular tubes. The distribution of the non-axisymmetric liquid film deposited on the wall should be investigated because of the film evaporation, which has the great influence on the heat transfer. In the present study, different height liquid film thickness in micro square channels are measured directly with the confocal method which is LDFM (laser focus displacement meter).

This paper demonstrates model for the calculation of pressure drop in gas-liquid slug flow consisting of single bubble and limited length liquid slug. Two-phase flow regime has resulted in first investigations of the hydrodynamics of such flow configuration. However, other hydrodynamic effects, such as pressure drop remain relatively unexplored completely. We measured the pressure drop of single bubble slug flow in microchannels and the relationship between the Experimental results and mechanism of pressure drop prediction is studied.

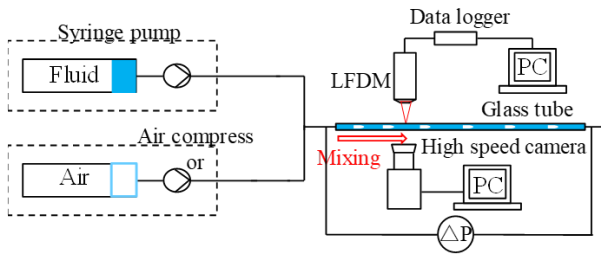
## 2 Experimental setup and procedures

In this part, two kinds of microchannel gas-liquid two-phase flow system are established. The transient measurement of liquid film thickness, pressure, bubble image and other signals is mainly carried out. The effects of physical properties, channel geometry, and mass flux on the flow pattern and the liquid film thickness of gas-liquid two-phase flow in a micro-channel are evaluated.

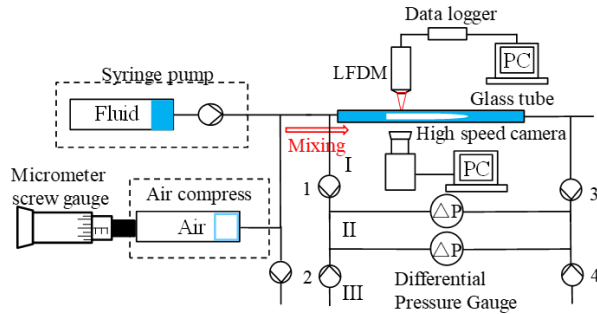
### 2.1 Experimental systems

The schematic diagram of the experimental apparatus is shown as Fig. 2.1(a). Water and air are injected by syringe pumps (Harvard Apparatus, accuracy within 0.35%, reproducibility within 0.05%), then they are mixed in the T-junction and introduced into the test section (circular Pyrex tube with diameter of 1mm). The flow pattern is recorded by high speed camera (Keyence, VW-600C), and the liquid film thickness is measured by laser confocal displacement meter (LCDM) (Keyence, LT9010). The resolution of LCDM is  $0.01\mu\text{m}$ , the response time is  $640\mu\text{s}$ , the diameter of the laser spot is  $2\mu\text{m}$ , and the focal length of the lens in the LCDM is about 5mm. Measured liquid film thickness is transformed to DC voltage signal in the range of  $\pm 10\text{ V}$ , and the data is transferred to a PC through the data logger. [3]

In order to further explore the influence of bubble dynamics of a single bubble, such as bubble length, bubble velocity and other factors on the liquid film thickness and pressure changes at both ends of the bubble in the two-phase flow process. The experimental equipment has been improved as follows. Gas bubble volume is controlled by a Micrometer screw gauge to quantify the length of a single bubble in the test section. (as shown in Fig.2.1(b))



(a) Syringe pump generated system



(b) Micrometer screw gauge generated system

Fig.2.1 Schematic diagram of the experimental setup

## 2.2 Test section and experimental procedure

Fig. 2.2 and 2.3 show the cross-section of the glass tube photographed with a digital microscope. In order to evaluate the influence of different channel sizes, shape and surface condition on the flow pattern observation experiment, four kinds of circular tubes with inner diameter of 0.24mm, 0.5mm, 0.76mm and 1.0mm, rectangular, curved and triangular channels with hydraulic diameter of 1.0mm were used.

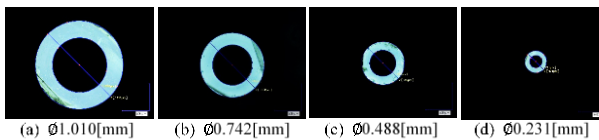
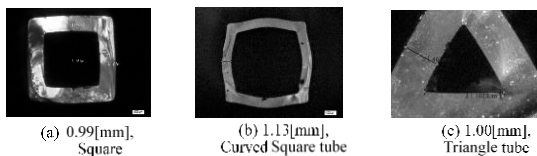
(a)  $\emptyset 1.010$ [mm] (b)  $\emptyset 0.742$ [mm] (c)  $\emptyset 0.488$ [mm] (d)  $\emptyset 0.231$ [mm]

Fig. 2. 2 Inner diameters of circular glass tubes.



(a) 0.99[mm], Square (b) 1.13[mm], Curved Square tube (c) 1.00[mm], Triangle tube

Fig. 2.3 Inner diameters of rectangular glass tubes.

In order to evaluate the effects of liquid properties on bubble velocity, pressure drop and liquid film thickness, three liquid phases with different viscosity and surface tension (water, ethanol, FC 72) were used. Table 2.1 shows the properties of fluid mentioned below.

Table 2.1 Properties of different fluids.

Fluid	$\rho$ [kg/m <sup>3</sup> ]	$\mu$ [ $\mu$ Pa·s]	$\sigma$ [N/m]
Water	997	889	72
Ethanol	785	1088	22.3
FC72	1680	672	12

## 3 Liquid Film Thickness for Gas-Liquid Two-Phase Flow

In this chapter, we conduct a lot of experiments in isothermal environment at first. This chapter mainly describes the dynamic characteristics of Taylor flow, such as film thickness, bubble velocity and void fraction.

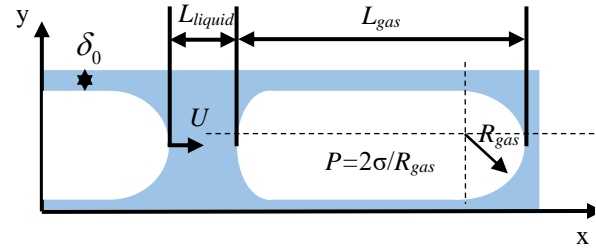


Fig. 3.1 Bubble velocity and liquid film of Taylor flow.

### 3.1 Taylor relation of liquid film thickness against capillary number

As shown in Fig. 3.1, during the forward flow of air bubbles at velocity  $U$ , a thin liquid film is formed on the wall of the channel. In the liquid film area under the bubble column, the gas-liquid interface presents a cylindrical distribution with a curvature of  $\kappa \approx 1/(R - \delta_0)$ , while in the tip of the bubble, the curvature of the gas-liquid interface is hemispherical  $\kappa \approx 2/(R - \delta_0)$ , where  $R$  represents the radius of the micro-channel,  $\delta_0$  is the initial thickness of the liquid film. Bretherton [4] calculated the initial liquid film thickness is as follow:

$$\frac{\delta_0}{R} \approx 0.643(3Ca)^{\frac{2}{3}}$$

Aussillous and Quere [5] then improved the formula of liquid film thickness, which is called Taylor relation:

$$\frac{\delta_0}{R} = 1.34Ca^{\frac{2}{3}} / (1 + 3.35Ca^{\frac{2}{3}})$$

### 3.2 Liquid film thickness of liquid-gas two phase flow inside microchannels

#### 3.2.1 Visualization of liquid-gas two phase flow

The liquid film thickness measurement and visualization experiments are carried out simultaneously. Bubble velocity and liquid film thickness correspond to each other. We try to find the relationship between them. Fig.3.2 shows the Taylor flow pattern of water/gas in different bubble velocity in the micro-channel with the diameter of 1.00 mm. It can be seen from the diagram that gas plug and liquid plug alternately occur in the Taylor flow. With the increase of bubble speed, the length of gas plug decreases and the shape of bubble head changes greatly.

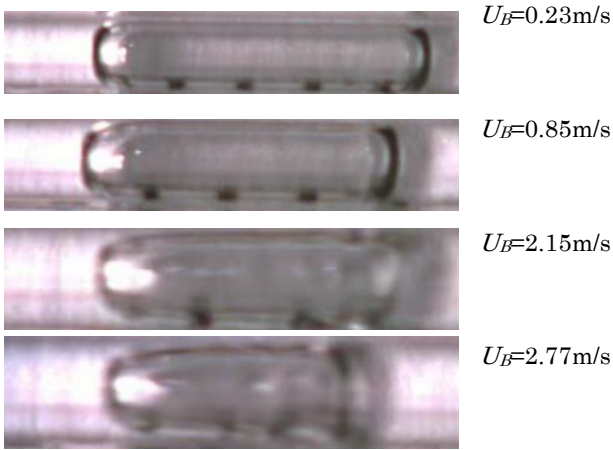


Fig. 3.2 Flow pattern of water/air gas-liquid two-phase flow in microchannels.

3.2.2 Time variation of liquid film thickness in different conditions

Fig.3.3 shows the typical measurement data of water in polygon channel at bubble velocity, 0.385m/s. we can see that the liquid film thickness in circular tube becomes nearly constant after the initial rapid decrease, which corresponds to the transition region between bubble nose and flat film region. Liquid film thickness is much thinner in square tube than that in the circular tube. what's more, liquid film in square tube continues to decrease with wavy fluctuations. frequency of the fluctuation decreases with time. Amplitude of the fluctuation is becoming smaller while the polygon counts increase and the curvature increase(Fig.3.4).

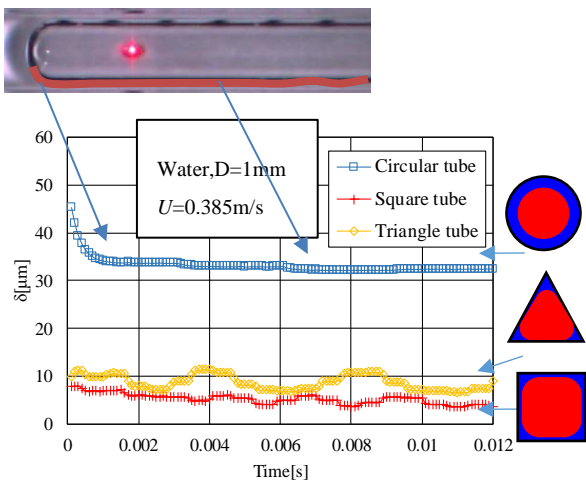


Fig. 3.3 Time variation of liquid film thickness in different tubes.(water/air, U=0.385m/s).

Fig.3.5 shows ethanol, FC-72 and water in square channel with bubble velocity of 0.331m/s. The trend of FC72 experiment was almost the same as that of ethanol experiment, because FC-72 also wetted quartz wall. On the contrary, in the water experiment, because water does not wet the quartz wall, part of the quartz wall becomes dry at the center of the channel.

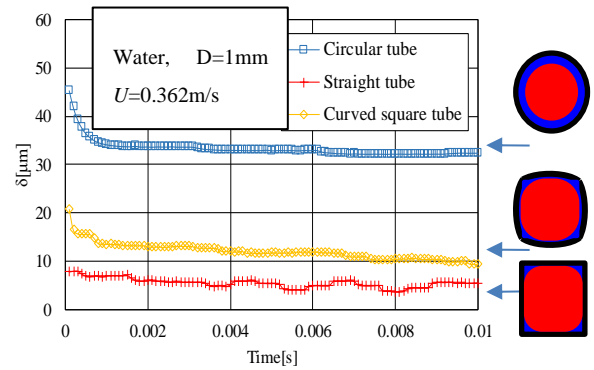


Fig. 3.4 Time variation of liquid film thickness in different tubes.(water/air, U=0.385m/s).

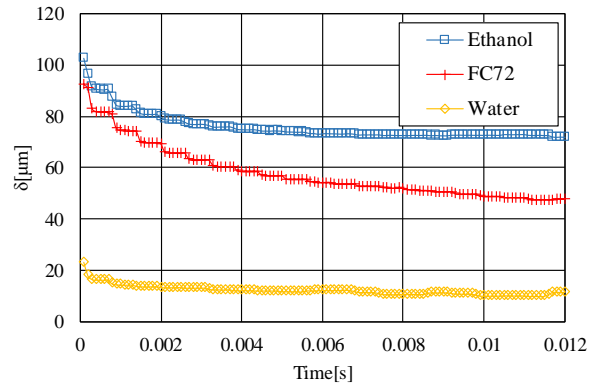


Fig. 3.5 Time variation of liquid film thickness in different liquids.(water/air, U=0.331m/s)

3.2.3 liquid film thickness against Capillary number

Fig. 3.6 shows that with the curvature become larger, the step increasing of liquid film becomes non-significant. Eventually convergent to the circular channel experiment.

Fig. 3.7 shows the interaction between initial liquid film thickness and bubble velocity in microchannels between water/gas, ethanol/gas, FC-72/gas, surface tension and viscosity is expressed by capillary number. The viscous force makes the liquid film thickness deposit thicker, the surface tension thins the liquid film thickness, the bubble velocity increases and the effect of viscous force increases.

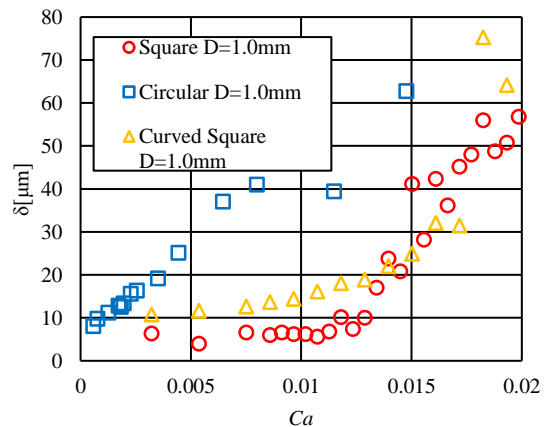


Fig. 3.6 Dimensionless liquid film thickness against Capillary number in different channels.

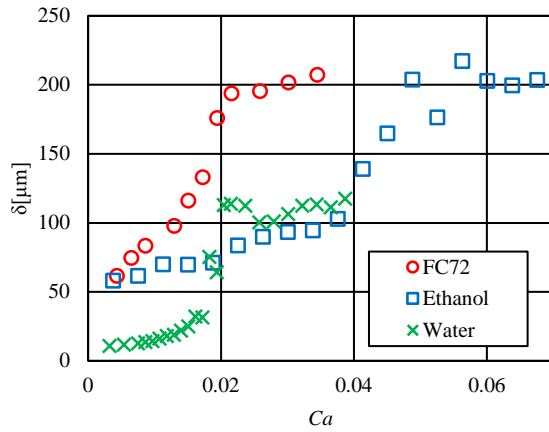


Fig. 3.7 Liquid film thickness against Capillary number in different working fluids inside rectangular tube.

#### 4 Liquid Film Thickness for Gas-Liquid Two-Phase Flow

##### 4.1 Mechanism of slug flow pressure drop inside microchannels

###### 4.1.1 Overall pressure drop along the single unit cell

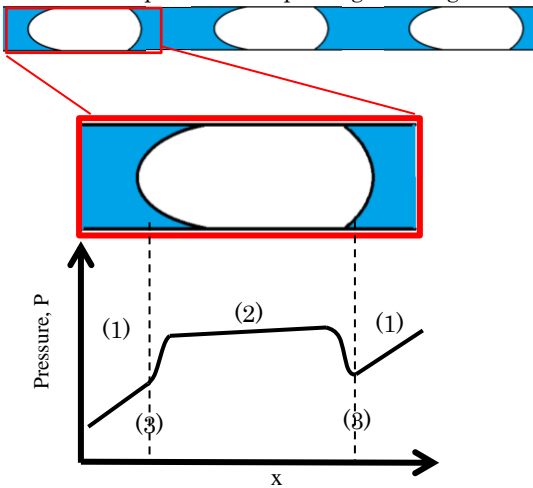


Fig. 4.1 Unit cell model of Pressure drop inside slug flow.

Fig.4.1 shows the unit cell model for investigate the contribution of pressure drop from this three regions:

- (1) In the liquid plug;
- (2) Along the body of the bubble;
- (3) Around the ends of the bubble;

With the measurement results from the visualization, the Theoretical Prediction of one bubble slug flow Pressure drop inside microchannels can be calculated as follow:

$$\Delta P = N[(\Delta P_{caps} + \Delta P_G) + \Delta P_l] = N[(\Delta P_{caps} + L_s \left(\frac{\partial P}{\partial x}\right)]$$

Where  $N=1$  is controlled by micrometer screw, and  $\Delta P_G$  can be negligible.

#### 4.2 Experimental Results against Theoretical Prediction

Fig.4.2 shows the Experimental Results for one bubble in 10cm length 1mm circular tube against Theoretical Prediction. It can be found from the experimental data that the pressure drop of two-phase flow of a single bubble has the same trend as that predicted by theory when  $Ca$  is about 0.001. When the flow rate increases, the experimental results are significantly higher than the predicted results because the predicted results neglect other resistance such as diameter-change resistance, gravity resistance and relative sliding friction between gas and liquid interface.

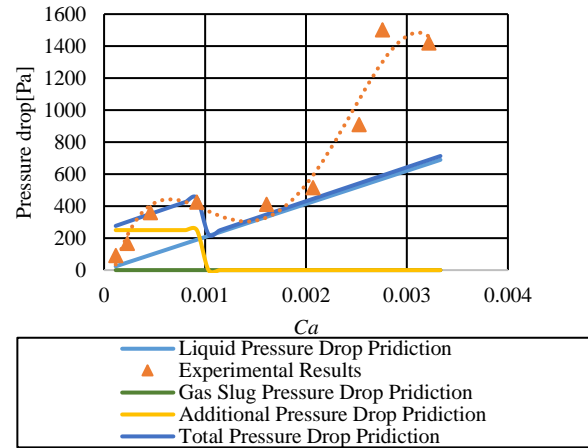


Fig. 4.2 Experimental Results of pressure drop against Theoretical Prediction. ( $D_h=1\text{mm}$ ,  $L=10\text{cm}$ )

#### 5 Conclusion

During the experimental investigation, the liquid film thickness and pressure drop of gas-liquid two-phase flow are mainly discussed.

We measured liquid film thickness inside several type of channels. And we can conclude that with the square tube curvature become evident, the step increasing of liquid film becomes non-significant.

The Pressure drop of single Bubble slug flow in microchannels is measured, and the relationship between the Experimental results and mechanism of pressure drop prediction is studied. It can be concluded from the experimental data that the pressure drop of two-phase flow of a single bubble has the same trend as that predicted by theory when  $Ca$  is about 0.001.

#### Reference

- 1) 吉永祐貴.日本冷凍空調学会, 2014, 31(4): 383-396.
- 2) Taha T.CES, 2006, 61(2): 665-675.
- 3) Kolb W B.CES, 1991, 46(9): 2181-2195.
- 4) Han Y. JSRAE Corp., (2010. 4).
- 5) Hazuku TExperiments in Fluids, 2005, 38(6): 780-788.
- 6) Suo M. Pressure drop in capillary slug flow[J]. 1968.
- 7) Nicholson M K. K. Chem. Eng, 1978, 56: 653-663.
- 8) Utaka Y.JHMT, 2009, 52(9):2205-2214.
- 9) Khandekar S. Heat Pipes, 2010, 1(023003): 1-20.